Multiple-electron capture and ionization in collisions of highly stripped ions with Ar atoms

A. Müller, B. Schuch, W. Groh, and E. Salzborn
University of Giessen, D-6300 Giessen, West Germany

H. F. Beyer and P. H. Mokler
GSI Darmstadt, D-6100 Darmstadt, West Germany

R. E. Olson
University of Missouri-Rolla, Rolla, Missouri 65401
(Received 7 October 1985)

Multiple-vacancy production in Ar atoms by 1.4-MeV/u highly stripped ion impact is studied. From a recoil-ion—projectile-ion coincidence experiment charge-state distributions of Ar ions were obtained distinguishing between pure ionization and capture of up to three electrons by $N^{6+,7+}$, $Fe^{12+,15+,20+,21+}$, Kr^{18+}, Gd^{37+}, and $U^{30+,36+,41+,44+,48+}$ ions. With increasing projectile charge state the relative abundances of multiply charged recoil ions increase. However, for high-charge-state projectiles, the relative fractions of recoil ions for concomitant electron capture and ionization are found to be independent of projectile charge or species. To interpret the data, classical trajectory Monte Carlo calculations have been made assuming the applicability of the independent-electron model. The calculations indicate the dominant electron capture is from the L-shell of Ar while the ionization process includes both the L- and M-shell electrons. The use of a common ionization potential inherent in the application of the independent-electron model is not adequate for the high degrees of ionization obtained in the investigated collisions; the cross sections for the production of high recoil-ion charge states are overestimated. Nevertheless, the calculated total cross sections for ionization and electron capture are in reasonable agreement with the available experimental data.

I. INTRODUCTION

Multiple-vacancy production in atomic collisions is of fundamental interest because it probes strong interactions between the projectile and the target electrons. Such reactions serve to severely test theoretical methods and approximations in the representation of this many-body collision problem. Also, since the interactions are strong the use of perturbation techniques in theoretical methods will generally be invalid.

The high probability of multiple ionization in close heavy-ion—atom encounters was first indicated by the observation of x-ray or Auger satellites (K^1L^n holes) and hypersatellites (K^2L^n) resulting from the decay of inner-shell vacancies produced in the collisions. Experimental results were explained on the basis of independent-particle models.[1,2] Slow highly stripped recoil ions were employed later to study atomic structures and atomic collisions[3,4] and low-energy beams of highly charged recoil ions were produced to investigate electron-capture processes.[5]

The interest in the production of slow highly charged recoil ions in fast heavy-ion—atom collisions as an alternative to the development of complicated ion sources has stimulated investigations of cross sections for multiple ionization of atoms by energetic ion impact.[6–9]

The present investigation tries to identify the physical mechanisms leading to multiple target ionization. Using both experiment and theory, partial cross sections $\sigma_{q,q-k}^{0,i}$ for the collision processes

$$A^{q+}+\mathrm{Ar}\rightarrow A^{(q-k)+}+\mathrm{Ar}^{i+}+(i-k)e \quad (1)$$

are determined for a specific energy of 1.4 MeV/u; i.e., fixed projectile velocity, with $k=0$, 1, 2, 3, and 4 and projectile ions ranging from N^{6+} to U^{48+}. This systematic study of the influence of projectile-ion charge and species on the recoil-ion charge-state distributions complements measurements of Kelbch *et al.*[9] on the effect of the projectile-ion energy.

II. THEORETICAL METHOD

The theoretical calculations use the classical-trajectory Monte Carlo (CTMC) method to determine the transition probabilities within a one-electron formalism and then extend these transition probabilities to represent a multielectron target atom by the use of the independent electron model.[10,11] We employ a three-body, three-dimensional CTMC method[12] that includes all forces between the incident ion, active electron, and target nucleus. The independent-electron model requires for validity that the collision be sudden, with the collision period sufficiently brief that the electrons cannot rearrange themselves during the collision. Hence, this model is only valid for collision velocities greater than the orbital velocities of the electrons being detached. The model ignores correlation effects between the electrons in a given shell, which should be a minor consideration for the collision processes under study here. More serious consideration must be

 ©1986 The American Physical Society

given, however, to the fact that a single ionization potential is inherently ascribed to all the electrons within a given shell. Thus, the importance of the higher stages of ionization from an electron shell will be overemphasized since in reality they are more tightly bound.

In the independent electron model, the transition probability for removing k of the K-shell electrons, l of the L-shell electrons, and m of the M-shell electrons is given by the simple product

$$P_{klm} = \binom{K}{k}(P_K)^k(1-P_K)^{K-k}\binom{L}{l}(P_L)^l(1-P_L)^{L-l} \times \binom{M}{m}(P_M)^m(1-P_M)^{M-m} . \quad (2)$$

In Eq. (2), $\binom{N}{n}$ is the binomial coefficient and P_n is the transition probability calculated as a function of impact parameter within a one-electron model. For the Ar target atom calculations presented here, we have included the L- and M-shell contributions to the total cross sections. An important characteristic of Eq. (2) is that unitarity is preserved in the calculational procedure. However, cascade effects after the collision, which tend to increase the multiple-ionization cross sections, are ignored.

Equation (2) is directly applicable to the calculation of the charge state of the recoil target ion, where the single-electron transition probabilities include the sum of the contributions from both electron capture and ionization. However, our interest lies in the determination of the simultaneous electron-capture—ionization events. For such a calculation, we have used the product of two equations of which each is given by (2) to determine the transition probabilities. The first component of such a formula employs the single-electron-capture transition probabilities, while the second component uses the ionization transition probabilities also calculated with the one-electron framework.

In order to obtain the one-electron transition probabilities, the CTMC method was employed. The calculational procedure for the CTMC method has previously been described in detail[12] and is based on solving Hamilton's equations of motion for a three-body system (18 coupled first-order differential equations). The coupled equations must be solved numerous times within the framework of the Monte-Carlo method to obtain an accurate description of the electron distribution about the target nucleus and to span the impact parameters required to describe the sollision. In the present calculations, 10 000 trajectories for each charge state and electron shell were adequate to determine transition probabilities of sufficient accuracy to employ the independent-electron model.

Since the CTMC method is only directly applicable to hydrogenic target atoms, it is necessary to extend the representation of the target electron so that it reproduces the dimensions of the electron shell under consideration. Such an extension requires that we determine an effective charge Z_{eff} of the target nucleus as seen by the active electron. We require that two conditions be met. The first is that the binding energy U of an electron in a shell be correct so that threshold energy behavior is accurately portrayed. The second condition is that the radial size of the simulated electron cloud must be reproduced so that the dimensions of the target atom are close to reality.

Within the confines of the classical hydrogenic model employed here, the above two conditions require that the expectation value of the active electrons be given by

$$\langle R \rangle = Z_{\text{eff}}/(-2U) , \quad (3)$$

where U is the electron binding energy in atomic units. In our calculations, we used the $\langle R \rangle$ Hartree-Fock values of Fischer[13] to determine Z_{eff}. The values of Z_{eff} used were 12.50 for the L-shell and 2.45 for the M-shell of Ar. Such values yield expectation values for the L- and M-shell of $0.38a_0$ and $1.60a_0$, respectively. It should be noted that because of the high-charge-states of the projectile ions, the collisions are of much longer range than indicated by the dimensions of the Ar target atom.[14]

In the calculations, we have assumed the projectile ion is fully stripped. Such an assumption gives rise to an underestimation of the ionization cross sections and an overestimation of the electron-capture cross sections when comparison is made to data from partially stripped ions in low stages of ionization. The reasons for the underestimation of the ionization cross sections for partially stripped ions are that we do not include the interactions of the projectile electrons with the target electrons and the fact that the target atom's electrons will see a higher effective charge for small impact-parameter collisions which penetrate the electron shells of the projectile. Conversely, the electron-capture cross sections may be overestimated since the electron capture to low-lying electron shells of the projectile can be blocked by resident electrons.

III. EXPERIMENT

The experiments were conducted at the GSI heavy-ion accelerator using one of the parasitic 1.4 MeV/u beam lines. The charge states of ions could be varied by introducing a foil stripper or a gas target upstream from the charge-state selecting magnet.

Figure 1 shows a schematic view of the experimental setup. A beam of momentum-analyzed ions A^{q+} is collimated by 0.5-mm-diam apertures to a maximum divergence of 1°. The ions then cross a thermal beam of Ar atoms emerging from a hollow needle. The recoil ions produced are extracted perpendicularly to the projectile beam by the electric field between two parallel plates which are typically on potentials ± 600 V. After passing a 5-mm-diam hole in the negatively biased plate and through a subsequent drift tube, the ions are postaccelerated and detected by a multichannel-plate detector with a coaxial anode. The grid in front of the channel plates rejects secondary electrons released by the ions and thus enhances the ion-detection efficiency. By variation of the ion energy it was shown that the relative detection efficiency is constant at energies ≥ 3 keV and slowly decreases as the ion energy is reduced (10% less at 2 keV). All apertures passed by the recoil ions are provided with 95% transparency grids, thus maintaining a plane geometry. The length of the drift tube is chosen to accomplish time-of-flight focusing of recoil ions produced

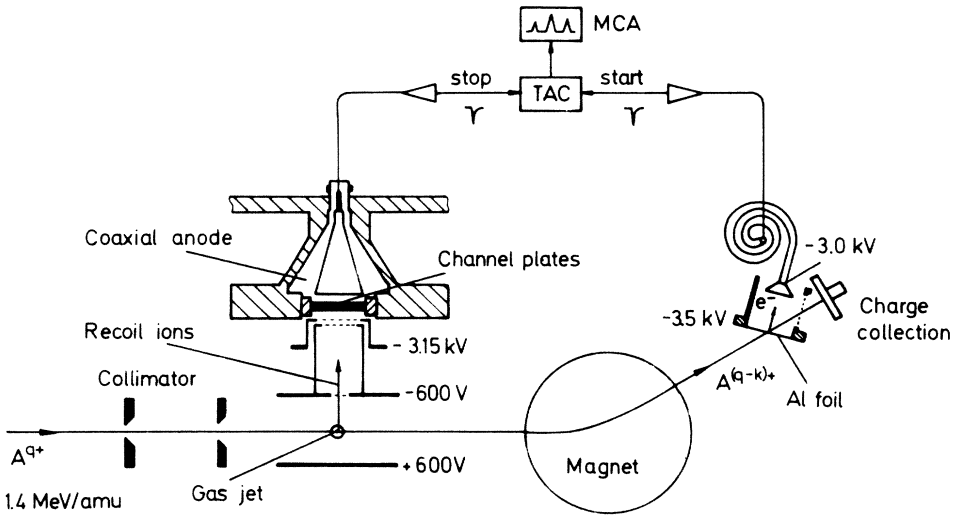

FIG. 1. Schematic of experimental setup (not to scale).

inside the condensor plates at different potentials because of the finite height of the projectile ion beam. The length of the drift tube is about equal to the distance between the condensor plates, i.e., 3 cm; final time focusing is reached after the acceleration to the channel-plate detector.

Uniform ion extraction, transmission, and detection for all charge states was ensured by comparison of measured recoil-ion charge-state spectra with results obtained by using a different but well-tested spectrometer described previously.[15]

The projectile ions, which may have changed their charge in or subsequent to the collision, are charge analyzed by a magnet. Ions in a given charge state $A^{(q-k)+}$ are passed through a thin Al foil which is biased with -3.5 kV. The ions are collected on a metal plate. When passing the Al foil the ions produce a shower of electrons which are accelerated to the entrance funnel of a channel electron multiplier providing the start pulse for a time-to-amplitude converter (TAC). The pulses initiated by the slow recoil ions in the multichannel plates stop the TAC. The recoil-ion time of flight is proportional to the square root $\sqrt{i}$ of its charge state. However, the projectiles all have the same (short) time of flight to their detector. Therefore, the time-of-flight spectrum yields the charge-state distribution of the recoil ions. This spectrum is automatically correlated to the final charge state of the projectiles, i.e, the number of electrons transferred in the collision.

Figure 2 shows a set of time-of-flight spectra obtained for Fe^{15+} projectiles colliding with Ar atoms. Spectrum 2(a) is obtained for pure ionization, i.e., the charge state of the projectile does not change during or after the collision. Charge states $i=1$, 2, and 3 are not displayed. The intensity rapidly increases as i decreases. Spectra 2(b), 2(c) and 2(d) result when the projectile picks up one, two, or three electrons from the AR target. The time resolution in these spectra is up to 500. Thus, a clear separation of recoil-ion charge states is possible. Problems with resolution may only arise for very high charge states produced by three-electron capture when the peaks become broader and are no longer completely separated.

The spectra shown in Fig. 2 as well as all other measurements were taken at low-target gas pressures with an estimated target thickness of 5×10^{-6} Torr cm. The reason for this severe restriction, which led to accumulation times of up to several hours for a measurement of capture with ionization, was the necessity to maintain single-collision conditions. The recoil ions must have little chance to reduce their charge by a second collision. However, the more severe problem was set by the projectiles; the cross sections for pure ionization are about 2 orders of magnitude larger than the cross sections for electron capture. Thus, a small fraction of projectile ions can capture an electron somewhere in the beam line *before* or *behind* the target chamber. These ions can produce recoil ions in an additional collision *in* the target without changing their charge and give a contribution to a spectrum thought to be for electron-capture processes even though they still fulfill the coincidence condition set by the magnetic charge-state analysis. The resulting recoil-ion charge-state spectrum is composed of two parts: a part with decreasing relative fractions as the charge state increases (typical for direct ionization) and a part with a bell-shaped distribution of ion charge states with a maximum at about $i=6$–10 (typical for electron-capture collisions). We made separate measurements for pure ionization where the recoil-ion charge-state spectrum is insensitive to the projectile-ion charge state, and the influence of multiple collisions is small. We then subtract the "pure ionization background" from a spectrum obtained with coincidences between recoil ions and charge-transferred projectiles, and thus obtain the desired distribution that is due to electron capture by the projectile. In order to keep

TABLE I. Typical total uncertainties ΔF_i of relative charge-state abundances measured.

F_i (%)	>40	5–40	<5
ΔF_i (%)	±4	±3	$=0.5F_i$

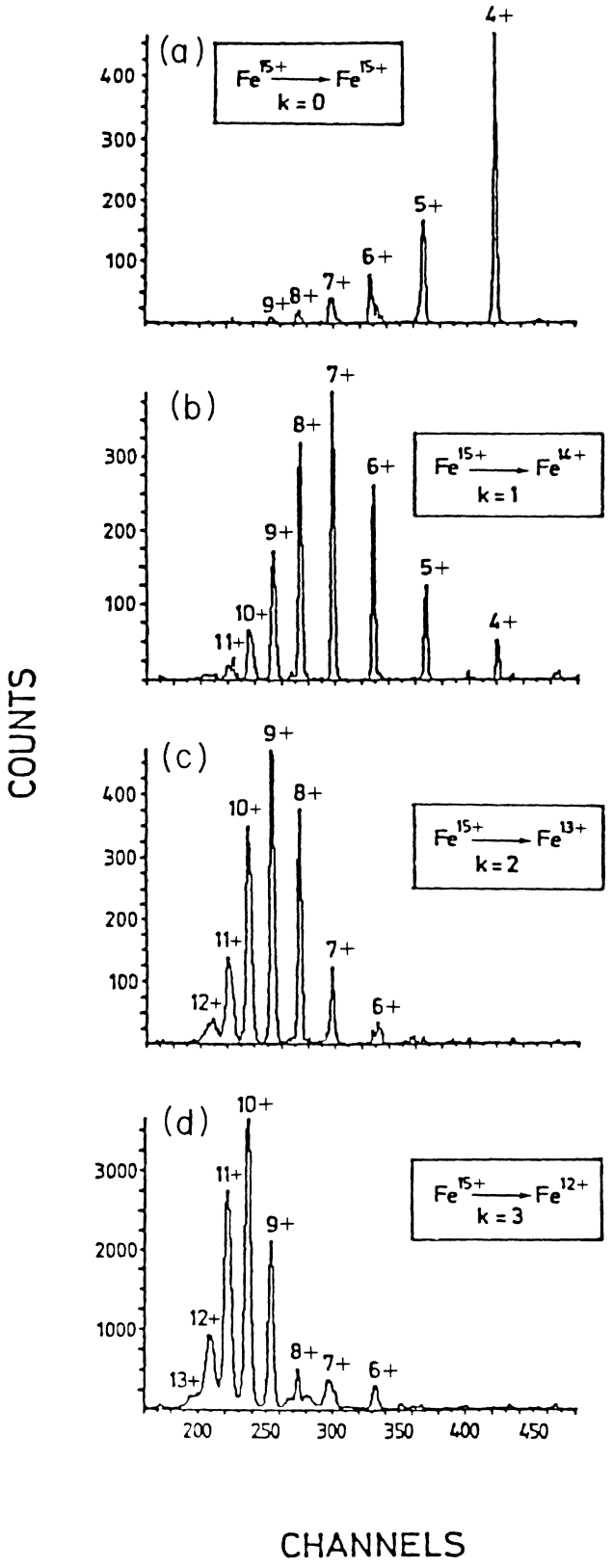

FIG. 2. Measured time-of-flight spectra of Ar^{i+} recoil ions produced in collisons $Fe^{15+}+Ar \rightarrow Fe^{(15-k)+}+Ar^{i+}+(i-k)e$ with $k=0,1,2,3$. For $k=0$ the peaks produced by Ar^{1+}, Ar^{2+}, and Ar^{3+} recoil ions are not displayed.

the necessary corrections small (i.e., no corrections necessary at charge states above the maximum of the distribution) we keep the target thickness near the low value mentioned above.

The remaining uncertainties in the relative charge-state fractions F_i of the Ar^{i+} recoil ions obtained, together with uncertainties due to random coincidence statistics, incomplete time resolution, and resulting difficulties in the integration of peaks lead to error bars which are usually related to the relative abundance of an ion charge state within the measured spectrum. Typical total uncertainties of relative charge-state abundances measured in this experiment are given in Table I.

IV. RESULTS

With the techniques described in the previous section relative abundances $F_i^{(k)}$ of Ar^{i+} recoil ions produced in collisions (Fig. 1) with $A^{q+}=N^{6+}$, N^{7+}, Fe^{12+}, Fe^{15+}, Fe^{20+}, Fe^{21+}, Kr^{18+}, Gd^{37+}, U^{30+}, U^{36+}, U^{41+}, U^{44+}, U^{48+} have been measured. The results obtained will be described in this section.

Figure 3 shows distributions of $F_i^{(k=0)}$ obtained when

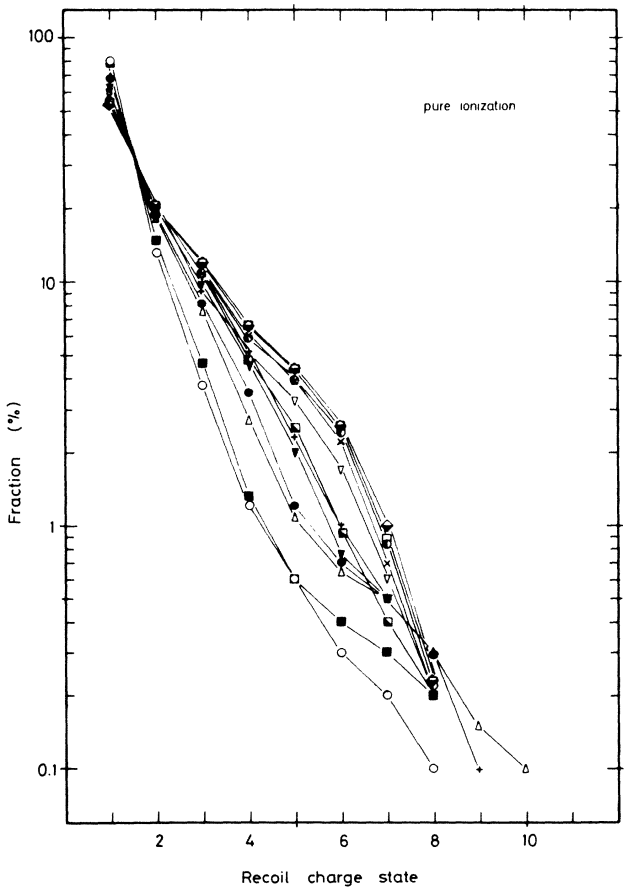

FIG. 3. Fractions F_i of recoil ions in different charge states produced in collisions $A^{q+}+Ar \rightarrow A^{q+}+Ar^{i+}+ie$. Projectile ion species are N^{6+} (○), N^{7+} (■), Fe^{12+} (△), Fe^{15+} (●), Fe^{20+} (+), Fe^{21+} (◪), Kr^{18+} (▼), Gd^{37+} (◇), U^{30+} (▽), U^{36+} (×), U^{41+} (◐), U^{44+} (□), U^{48+} (◆). The specific energy is 1.4 MeV/u.

the projectiles do not change their charge in the collision (pure ionization of the Ar target atom). With increasing charge state i of the recoil ions the relative abundances F_i rapidly decrease especially for the projectiles N^{6+} and N^{7+}. There is indication for an enhanced relative efficiency for multiple ionization by projectiles with higher charge states, however, the relative abundance of Ar^{7+} produced by U^{48+} is not more than four times that produced by N^{6+} (of course the absolute cross section for the production of Ar^{7+}, $\sigma_{q,q}^{0,i}$, is much higher with U^{48+} than with N^{6+}; see Sec. V).

For collisons where the projectile changed its charge from q to $q-1$ when observed long after the collision ($\sim 10^{-7}$ sec terms one-electron capture in this paper) the trend of comparatively little effect of the projectile charge state on the fractions $F_i^{(k)}$ is continued except for the very low charge states. Figure 4 displays the measured relative abundances $F_i^{(k=1)}$ of Ar^{i+} recoil ions for one-electron capture as a function of i. N^{6+} and to less extent also Fe^{12+} produce broader charge-state distributions which are shifted to lower values of i while all other projectiles produce very similar distributions with a maximum at about $i=7$.

For collisions with the capture of $k=2$, 3, or 4 electrons only a few charge-state distributions were measured. The results obtained are shown in Fig. 5. The maximum of the charge-state distributions for multiple-electron capture is shifted from $i=7$ for $k=1$ to $i=9$ for $k=2$, $i=10$ for $k=3$, and $i=11$ for $k=4$. Apparently there is a discontinuity in this shift: $\Delta i=2$ between $k=1$ and $k=2$ while $\Delta i=1$ in all other cases.

The relative abundances of recoil ions obtained by this experiment can be normalized to total cross sections, to determine absolute partial cross sections $\sigma_{q,q-k}^{0,i}$ for processes described by Eq. (1). Total cross sections for net ionization and electron capture by fast highly-charged ions have been systematically investigated by Schlachter *et al.*[16] Scaling rules have been extracted from the data to reproduce total cross sections within a factor of 2. At 1.4 MeV/u Erb[17] has measured total electron-capture cross sections $\sigma_{q,q-k}$ with $k=1,2,3$ for projectiles in charge states $q=22$–47. The available experimental data show that the total net ionization cross sections measured by Schlachter *et al.*[16]

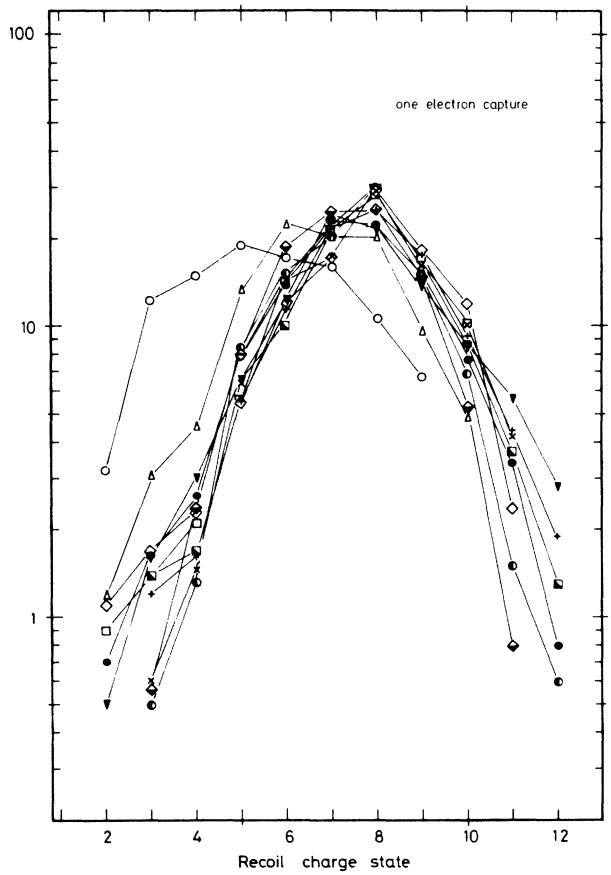

FIG. 4. Fractions F_i of recoil ions in different charge states produced in collisons $A^{q+}+Ar \rightarrow A^{(q-1)+}+Ar^{i+}+(i-1)e$. For projectile ion symbols see Fig. 3. The specific energy is 1.4 MeV/u.

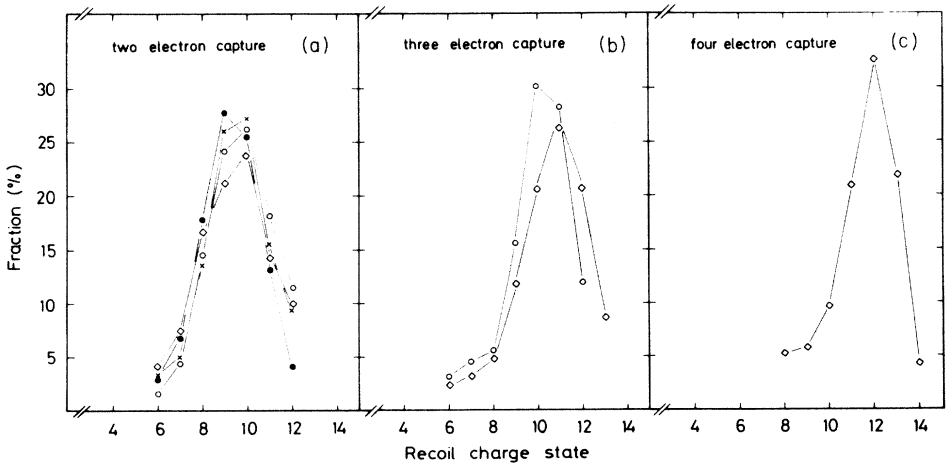

FIG. 5. Fraction F_i of recoil ions in different charge states produced in collisons $A^{q+}+Ar \rightarrow A^{(q-k)+}+Ar^{i+}+(i-k)e$ for (a) $k=2$, (b) $k=3$, and (c) $k=4$. Projectile ion species are Fe^{12+} (●), Fe^{15+} (○), Gd^{37+} (×), U^{44+} (◇). The specific energy is 1.4 MeV/u.

$$\sigma_q^{\text{ion}}=\sum_i i\sigma_q^{0,i}=\sum_i i\sum_k \sigma_{q,q-k}^{0,i} \tag{4}$$

have only minute contributions from electron capture and stripping at the present energies: $\sigma_{q,q-k}<0.01\sigma_q^{\text{ion}}$, so that

$$\sigma_q^{\text{ion}}=\sum_i i\sigma_{q,q}^{0,i} \tag{5}$$

is a good approximation. The absolute partial cross sections for pure multiple ionization can then be determined from the present relative charge-state abundances $F_i^{(k=0)}$ of target ions. Since

$$F_i^{(k=0)}=\sigma_{q,q}^{0,i}\Big/\sum_i \sigma_{q,q}^{0,i}\ , \tag{6}$$

it follows that

$$\sigma_{q,q}^{0,i}=F_i^{(k=0)}\sigma_q^{\text{ion}}\Big/\sum_i iF_i^{(k=0)}\ . \tag{7}$$

The accuracy of the partial cross sections is mainly limited by the uncertainty of absolute σ_q^{ion} data and the increased experimental uncertainties of small fractions $F_i^{(k=0)}$ obtained in the present experiment.

In the case of electron capture by the fast projectile, the desired absolute partial cross sections $\sigma_{q,q-k}^{0,i}$ $(k\geq 1)$ follows directly from the total cross sections $\sigma_{q,q-k}$ when the relative charge-state abundances from the present experiment are used:

$$\sigma_{q,q-k}^{0,i}=F_i^{(k=1)}\sigma_{q,q-k}\ . \tag{8}$$

V. DISCUSSION

A presentation of experimental and calculated results for $q=5$–25 is given in Figs. 6 and 7. For charge states $q=12$, 15, and 20 a direct comparison can be made between theory and experiment (Fe^{12+}, Fe^{15+}, and Fe^{20+} projectile ions in the experiment). The agreement can only be considered to be qualitative, but cognizance should be given to the fact that the processes under study are a complicated many-body problem involving the interplay between discrete and continuum levels. Also, the theory is predictive in nature and does not use adjustable parameters to fit the data.

The general trend observed in the calculations is that the single- and multiple-electron-capture events involve a collision process where numerous electrons are simultaneously ejected into the continuum. For the Ar target atom, the electron capture process primarily involves capture of L-shell electrons. The electrons which are ionized come mainly from the outer M shell, and to a lesser extent from the L shell. As shown in the experimental data for single-electron capture in Fig. 4, the recoil-ion charge state maximizes around 8 + for all projectile ions with $q\gtrsim 10$. The $q=5$ calculations, Fig. 6, place the maximum value for the recoil-ion charge state at 4 +, which is in agreement with the trend observed in the experimental data for N^{6+}, Fig. 4.

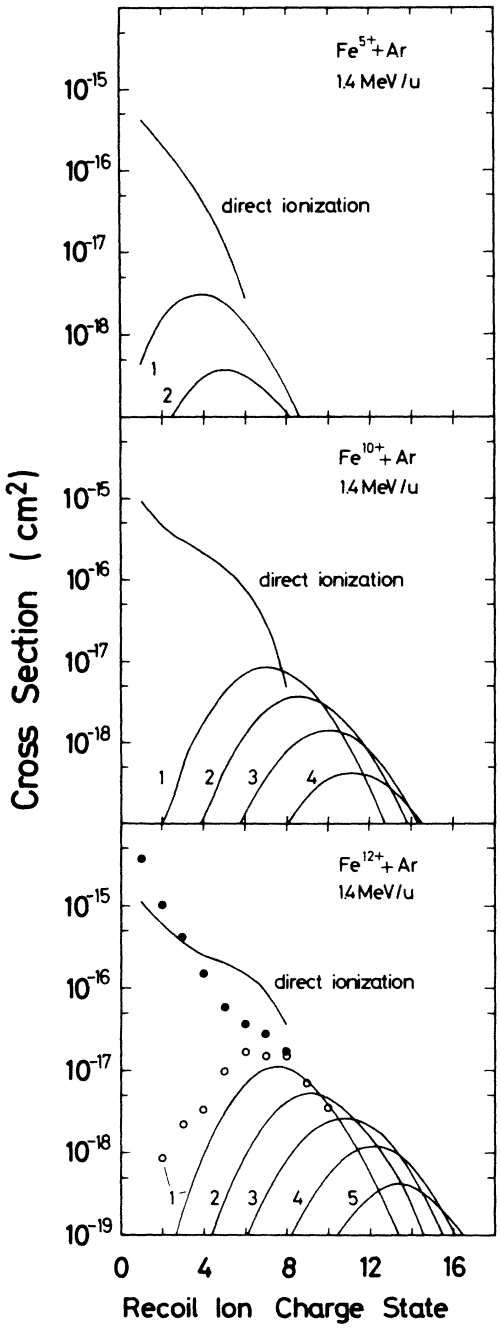

FIG. 6. Cross sections $\sigma_{q,q-k}^{0,i}$ for direction ionization $(k=0)$ and capture of $k=1$, 2, 3, 4, or 5 electrons in 1.4 MeV/u collisions of Fe^{5+}, Fe^{10+}, and Fe^{12+} ions with Ar atoms. Theoretical calculations are represented by smooth solid curves. Experimental data were taken for Fe^{12+} ions and $k=0$ and $k=1$.

Multiple-electron-capture events display slightly decreasing cross sections and shifts to higher values of the recoil-ion charge state. The shifts to higher recoil-ion charge states are not dramatic, with the increment being only 1.0 + to 1.5 +, for each succeeding capture of an electron. Such a trend is in agreement with the experimental results. The reason for such a small shift is that the single- and multiple-electron-capture events from the

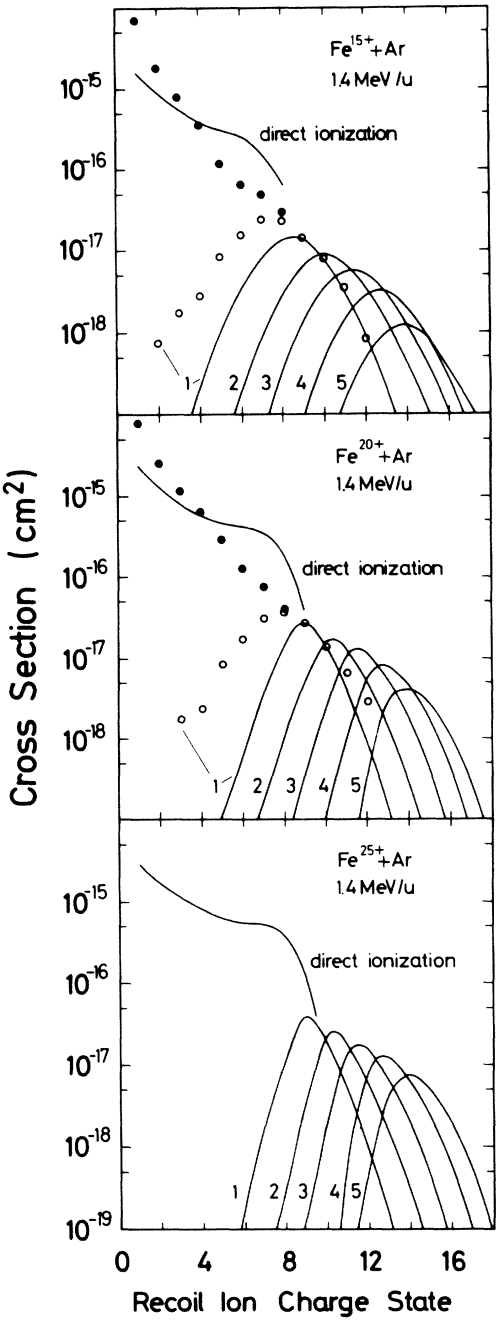

FIG. 7. Cross sections $\sigma^{0,i}_{q,q-k}$ for direction ionization ($k=0$) and capture of $k=1$, 2, 3, 4, or 5 electrons in 1.4 MeV/u collisions of Fe^{15+}, Fe^{20+}, and Fe^{52+} ions with Ar atoms. Theoretical calculations are represented by smooth solid curves. Experimental data were taken for Fe^{15+}, Fe^{20+} ions and $k=0$ and $k=1$.

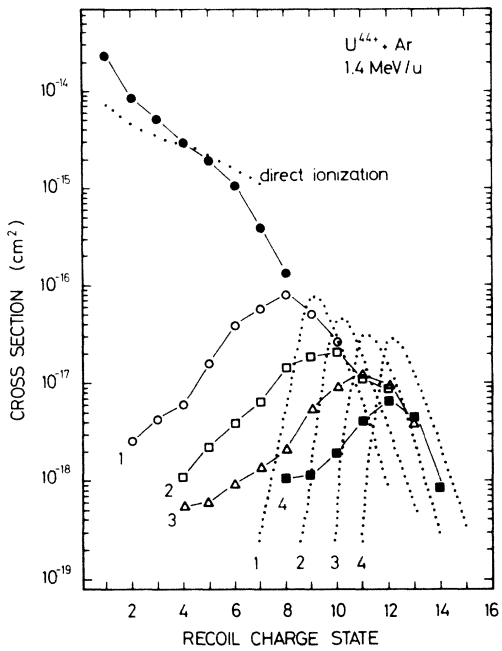

FIG. 8. Cross sections $\sigma^{0,i}_{q,q-k}$ for direct ionization ($k=0$) and capture of $k=1$, 2, 3, or 4 electrons in 1.4 MeV/u collisions of U^{44+} ions with Ar atoms. Theoretical calculations are represented by dotted lines. The experimental charge-state fractions F_i measured for U^{44+} ions with $k=4$ were normalized to a total 4-electron-capture cross section obtained by extrapolating data for $k=1$, 2, and 3 measured by Erb (Ref. 17).

L-shell occur in the same region of impact-parameter space where the M-shell electrons have essentially all been ionized. The capture of a succeeding larger number of electrons thus requires only a slightly smaller impact parameter with little change in the number of electrons that are ionized.

A direct comparison between theory and experiment for single- and multiple-electron capture is shown in Fig. 8. Experimental data were obtained for U^{44+} projectile ions. The positions of the maxima in the recoil-ion charge state after electron capture are reasonably portrayed by the calculations. However, the widths of the calculated recoil-ion charge-state peaks are in poor accord with experiment. In particular, the U^{44+} calculations predict much narrower peaks than observed, even though the peak maxima are in fair agreement. One possible explanation for the difference is that autoionization mechanisms have not been included in the theoretical description. In particular, multiple-electron capture by U^{44+} will proceed into excited electronic levels which can radiatively relax to the ground state or Auger ionize. In the latter case the recoil-ion spectra will be broadened. Likewise, the target atom can autoionize if several electrons are left in excited levels after the collision.

The absolute magnitude of the total-electron-capture cross sections agree within a factor of 3 with experiment. For single-electron capture, theory agrees well with the scaling formula of Schlachter *et al.*[18] for $q \lesssim 15$. For higher charge states, the theoretical values become increasingly inaccurate although a factor-of-2 agreement is realized for $q=25$.

There are few data for multiple-electron capture to test the theoretical procedures. As a prediction, we would expect theory to overestimate the cross sections because final-state rearrangements have not been included. In particular, multiple-electron capture into an excited level will lead to autoionization as the ion relaxes to its ground-state configuration. The few existing experimental data points tend to confirm this trend.

[1]J. H. McGuire and P. Richard, Phys. Rev. A **8**, 1374 (1973).
[2]R. L. Kauffman, C. W. Woods, K. A. Jamison, and P. Richard, Phys. Rev. A **11**, 872 (1975).
[3]R. Mann, F. Folkmann, and H. F. Beyer, J. Phys. B **14**, 1161 (1981).
[4]H. F. Beyer, R. Mann, F. Folkmann, and P. H. Mokler, J. Phys. B **15**, 3853 (1982).
[5]R. Mann, C. L. Cocke, A. S. Schlachter, M. Prior, and R. Marrus, Phys. Rev. Lett. **49**, 1329 (1982).
[6]C. L. Cocke, Phys. Rev. A **20**, 749 (1979).
[7]T. J. Gray, C. L. Cocke, and E. Justiniano, Phys. Rev. A **22**, 849 (1980).
[8]A. S. Schlachter, W. Groh, A. Müller, H. F. Beyer, R. Mann, and R. E. Olson, Phys. Rev. A **26**, 1373 (1982).
[9]S. Kelbch, R. Mann, P. Richard, H. Schmidt-Böcking, and J. Ullrich, J. Phys. B **18**, 323 (1985).
[10]J. M. Hansteen and O. P. Mosebekk, Phys. Rev. Lett. **29**, 1361 (1972).
[11]J. H. McGuire and L. Weaver, Phys. Rev. A **16**, 41 (1977).
[12]R. E. Olson and A. Salop, Phys. Rev. A **16**, 531 (1977).
[13]C. F. Fischer, *The Hartree-Fock Method for Atoms* (Wiley, New York, 1977), p. 34.
[14]R. E. Olson, J. Phys. B **12**, 1843 (1979).
[15]W. Groh, A. Müller, A. S. Schlachter, and E. Salzborn, J. Phys. B **16**, 1997 (1983).
[16]A. S. Schlachter, K. H. Berkner, W. G. Graham, R. V. Pyle, P. J. Schneider, K. R. Stalder, J. W. Stearns, J. A. Tanis, and R. E. Olson, Phys. Rev. A **23**, 2331 (1981).
[17]W. Erb, Thesis, Darmstadt, 1978 [GSI-Bericht P-7-78 (available from Gesellschaft für Schwerionenforschung mbH, Postfach 110 541, D-6100 Darmstadt)].
[18]A. S. Schlachter, J. W. Stearns, W. G. Graham, K. H. Berkner, R. V. Pyle, and J. A. Tanis, Phys. Rev. A **27**, 3372 (1983).